Raman, Infrared, and Circular Dichroism Spectroscopic Studies on Metallothionein: A Predominantly "Turn"-Containing Protein†

J. Pande,*,‡,§ C. Pande,§ D. Gilg,‡ M. Vašák,‡ R. Callender,§ and J. H. R. Kägi‡

Biochemisches Institut der Universität Zürich, CH-8057 Zürich, Switzerland, and Department of Physics, City College of the City University of New York, New York, New York 10031

Received March 25, 1986

ABSTRACT: Raman and IR spectra of rabbit liver metallothionein 1 (MT-1) containing 7 mol of either cadmium or zinc ions reveal high-lying amide III bands between 1290 and 1330 cm^{-1}, indicative of β-turns. A comparison of the splitting pattern in the amide III region below 1290 cm^{-1} and in the amide I band between 1600 and 1700 cm^{-1}, with the normal-mode calculations of Lagant et al. [Lagant, P., Vergoten, G., Fleury, G., & Loucheux-Lefebvre, M. (1984a) *Eur. J. Biochem. 139*, 137–148; Lagant, P., Vergoten, G., Fleury, G., & Loucheux-Lefebvre, M. (1984b) *Eur. J. Biochem. 139*, 149–154; Lagant, P., Vergoten, G., Fleury, G., & Loucheux-Lefebvre, M. (1984c) *J. Raman Spectrosc. 15*, 421–423] and Krimm and Bandekar [Krimm, S., & Bandekar, J. (1980) *Biopolymers 19*, 1–29], suggests that metal-bound (holo) MT-1 consists largely of β-turns of type II. In contrast, the metal-free (apo) protein displays a predominantly unordered conformation. The Raman spectra of the holoproteins below 1000 cm^{-1} are characterized by several unusual skeletal stretching and bending modes. The spectral pattern between 760 and 800 cm^{-1} in conjunction with the splitting of the amide I band agrees closely with the normal-mode calculations of Lagant et al. (1984b) on model peptides and is indicative of the presence of type III β-turns (or 3_{10}-helical segments) in MT-1. The good agreement between the vibrational spectroscopic results presented here on MT-1 and the 2D NMR solution structure and X-ray crystal structure data on MT-2 [Braun, G., Wagner, G., Wörgötter, E., Vašák, M., Kägi, J. H. R., & Wüthrich, K. (1986) *J. Mol. Biol. 187*, 125–129; Wagner, G., Neuhaus, D., Wörgötter, E., Vašák, M., Kägi, J. H. R., & Wüthrich, K. (1986) *J. Mol. Biol. 187*, 131–135; Furey, W. F., Robbins, A. H., Clancy, L. L., Winge, D. R., Wang, B. C., & Stout, C. D. (1986) *Science (Washington, D.C.) 231*, 704–710] demonstrates that both isoforms of the protein assume nearly identical folding patterns.

Tight turns in proteins have long been recognized as important elements of secondary structure (Richardson, 1981). The definition of turns has, however, been considerably modified and expanded to include several variations of the main scheme first proposed by Venkatachalam (1968). In its most general sense, a turn is said to be generated whenever a polypeptide chain changes direction. A β-turn, more specifically, consists of a four amino acid residue segment with or without an internal hydrogen bond (Rose et al., 1985). Among the physical methods suitable for the characterization of turns in peptides and proteins are X-ray crystallography and 2D NMR, circular dichroism (CD), and vibrational spectroscopies, with the first two techniques being better suited for the unambiguous identification of the type of turn. The application of IR and Raman spectroscopies to the detection of turns in peptides has in recent years been enormously facilitated by the theoretical predictions of the normal-mode frequencies for β-turns of various types (Krimm & Bandekar, 1980; Lagant et al., 1984a,b). Several small peptides have been examined by Raman and/or IR spectroscopy and the data compared with theoretical predictions, with varying degrees of success [Lagant et al. (1984b) and references cited therein; Bandekar et al., 1982; Holosi et al., 1985]. However, to our knowledge there are no detailed data available in the literature that substantiate the theoretical predictions with experimental results, for larger peptides and proteins.

Metallothioneins (MTs) are small metal-binding proteins distinguished by the predominance of cysteine residues and the total absence of aromatic residues in their amino acid sequence. The polypeptide chain is characteristically interspersed with CXC, CXXC, and CXXXC units, where C denotes cysteine and X denotes any other amino acid, such that all 20 cysteine residues bind maximally seven Zn(II) ions in the native state (Nordberg & Kojima, 1979). The protein is inducible by several metal ions, particularly Zn(II), Cd(II), Hg(II), and Cu(I), and binds these ions in varying stoichiometries (Kägi et al., 1984). The entire metal content is distributed into two clusters consisting of four and three metal ions (Otvos & Armitage, 1980), and in the cadmium- and zinc-containing proteins, each metal ion is coordinated tetrahedrally to terminal and bridging cysteine sulfurs (Vašák & Kägi, 1983). The main contribution to the secondary structure of MT was predicted earlier from the amino acid sequence (Boulanger et al., 1983; Gilg, 1985) to arise from β-turns, to the near exclusion of α-helical and extended β-sheet segments. These predictions have now been confirmed for the cadmium-induced protein from rat liver, with a stoichiometry of Cd_5Zn_2, by the X-ray crystallographic map at 2.3-Å resolution (Furey et al., 1985), and in solution for the rabbit liver protein reconstituted in vitro with seven Cd(II) ions, by 2D NMR spectroscopy (Wagner et al., 1986; Braun et al., 1986). In this paper, we present the first Raman and IR results on this predominantly "turn"-containing protein in its metal-free (apo)

† This work was supported in part by Swiss National Science Foundation Grant 3.207.82 to J.H.R.K., National Institutes of Health Grant GM 35183 to R.C., and a short-term EMBO fellowship to J.P.

* Address correspondence to this author at City College of the City University of New York.

‡ Biochemisches Institut der Universität Zürich.

§ City College of the City University of New York.

0006-2960/86/0425-5526$01.50/0

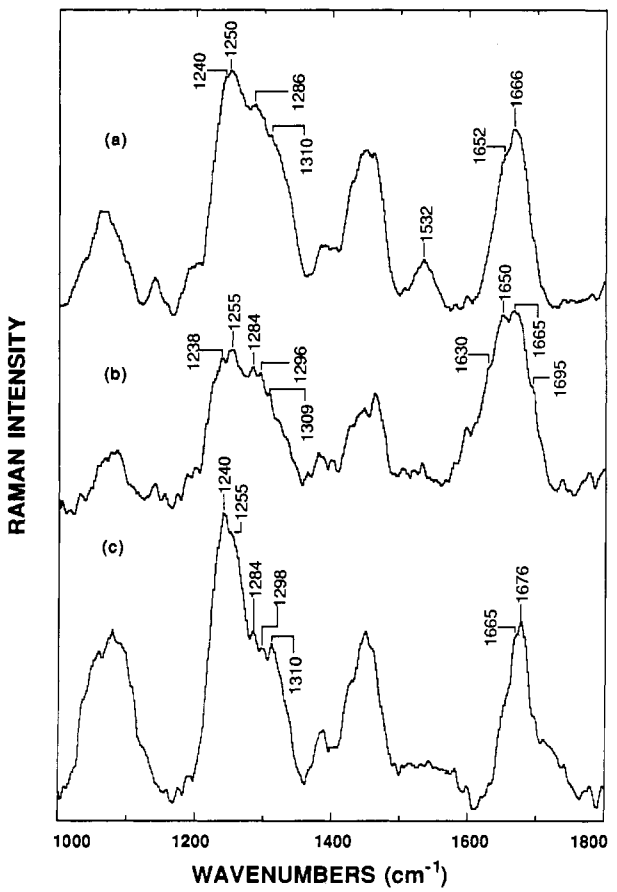

FIGURE 1: Raman spectra of (a) Zn_7-, (b) Cd_7-, and (c) apoMT-1 in aqueous 25 mM Tris buffer, pH 8.6 (a and b) and pH 1.7 (c): laser excitation at 488 nm; sample temperature 4 °C.

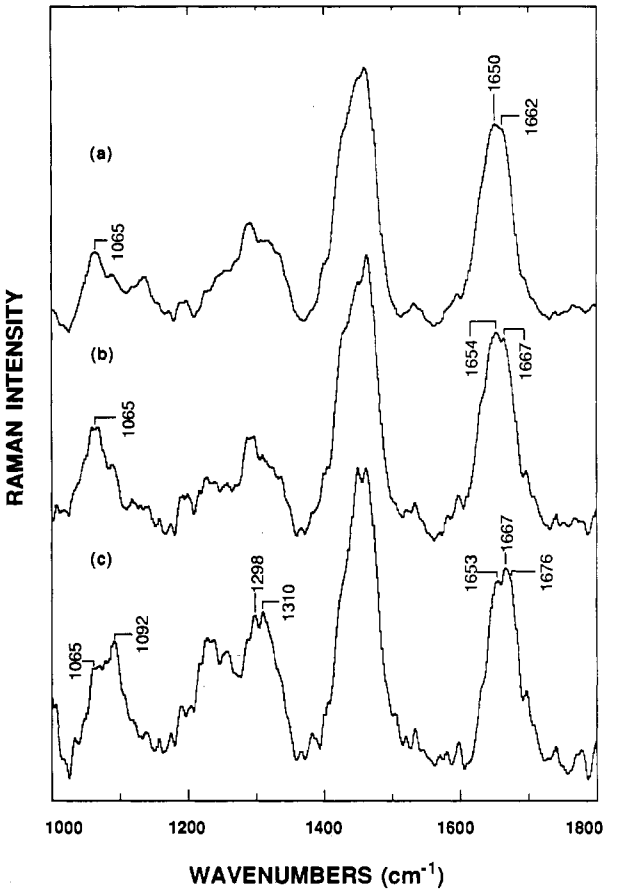

FIGURE 2: Raman spectra of (a) Zn_7-, (b) Cd_7-, and (c) apoMT-1 in deuterated 25 mM Tris buffer, pD 8.6 (a and b) and pD 1.7 (c). Experimental conditions as in Figure 1.

and two of its metal-bound (holo) forms and evaluate the data in the light of the theoretical normal-mode predictions on model peptides.

Materials and Methods

Native MT-1 from rabbit liver was isolated as described elsewhere (Kimura et al., 1979). In vitro reconstituted zinc and cadmium MT-1, each containing 7–7.5 mol equiv of either metal ion/mol of protein (i.e., Zn_7- and Cd_7-MT-1), and the apoprotein were prepared according to established procedures (Vašák & Kägi, 1983). The final material was resubjected to gel filtration over Sephadex G-50 to minimize dimer contribution if any. Deuterated samples were prepared by repeated lyophilization in D_2O (pD 8.6 for holoMTs and 1.7 for apoMT).

Raman spectra were obtained on a Spex Model 1877 triplemate spectrometer, with 488-nm excitation from a Spectra Physics Model 165 argon ion laser. Typical power levels at the sample averaged about 150 mW. A total of 80–100 μL of the sample at a concentration of 10 mM in 25 mM aqueous or deuterated Tris [tris(hydroxymethyl)aminomethane] buffer was placed in a 3 × 3 mm glass cuvette thermostated at ~4 °C. Scattered radiation at 90° to the incident beam was detected by an OMA system consisting of a thermoelectrically cooled solid-state detector/controller assembly (EG & G Princeton Applied Research Model 1420-2/1218).

Data were accumulated and analyzed on an LSI-11 microcomputer from Digital Equipment Corp., interfaced to the multichannel Raman detection system. All spectra were calibrated against the Raman lines of toluene and between 1000 and 1700 cm^{-1} normalized with respect to a constant number of counts in the amide I region.

Infrared spectra of thin films of MT were obtained on CdTe reflection plates by attenuated total reflection (ATR), on a Perkin-Elmer PE 225 IR spectrophotometer, under nitrogen. The films were prepared by drying aqueous solutions of native (Cd_5,Zn_2)-MT in dilute carbonate buffer, pH 9.5, and apoMT in 20 mM HCl, pH 1.7, on the reflection plates. Solution spectra in D_2O were obtained in the amide I′ region in CaF_2 cells on a Beckman 20A IR spectrophotometer, with a spectral bandwidth of 1–2 cm^{-1}. CD spectra were obtained on Cary 61 and Jasco J-40 AS spectropolarimeters. The data are expressed as mean residue ellipticity.

Results

The region of the Raman spectrum between 1200 and 1330 cm^{-1}, typically called the amide III region, is shown in Figure 1 for the Zn_7, Cd_7, and apo derivatives of MT in aqueous buffer. In the two holoproteins, this region is dominated by intense lines ranging from 1240 to 1260 cm^{-1} and 1280 to 1310 cm^{-1}, all of which are of comparable intensity (Figure 1a,b), whereas for apoMT (Figure 1c) the lines between 1240 and 1260 cm^{-1} are nearly twice as intense as those at higher frequencies. The results following sample deuteration are shown in Figure 2. The spectra of both holoproteins (Figure 2a,b) are characterized by a substantial drop in intensity compared to those in aqueous buffer in the entire 1240–1330-cm^{-1} region. In the case of apoMT, there is a considerable intensity drop around 1240–1260 cm^{-1} and some loss near 1280 cm^{-1}, but more significantly, the doublet around 1300 and 1310 cm^{-1} is virtually unaltered.

Differences between the metal-containing and metal-free forms are also evident in the amide I region of the spectra between 1600 and 1700 cm^{-1}, in aqueous buffer (Figure 1).

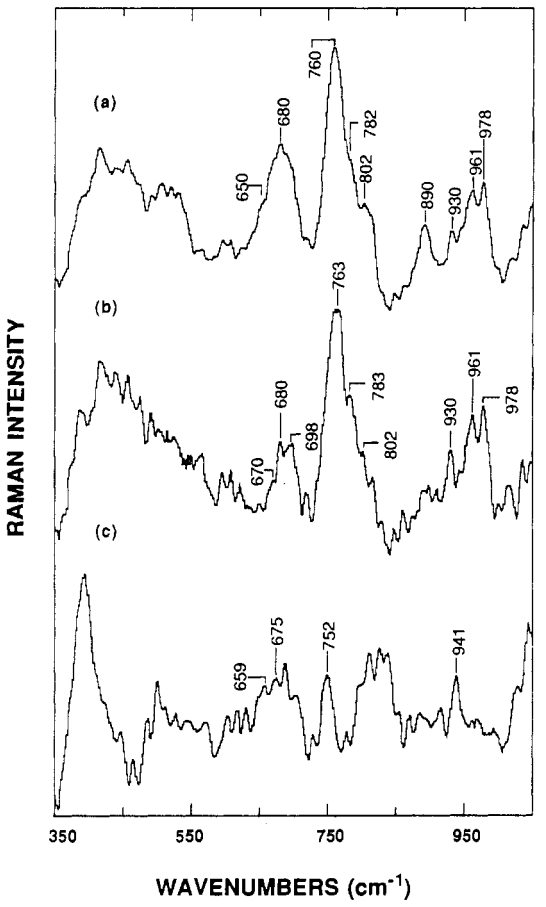

FIGURE 3: Raman spectra of (a) Zn_7-, (b) Cd_7-, and (c) apoMT-1 in aqueous 25 mM Tris buffer, pH 8.6 (a and b) and pH 1.7 (c): laser excitation at 488 nm; sample temperature 4 °C.

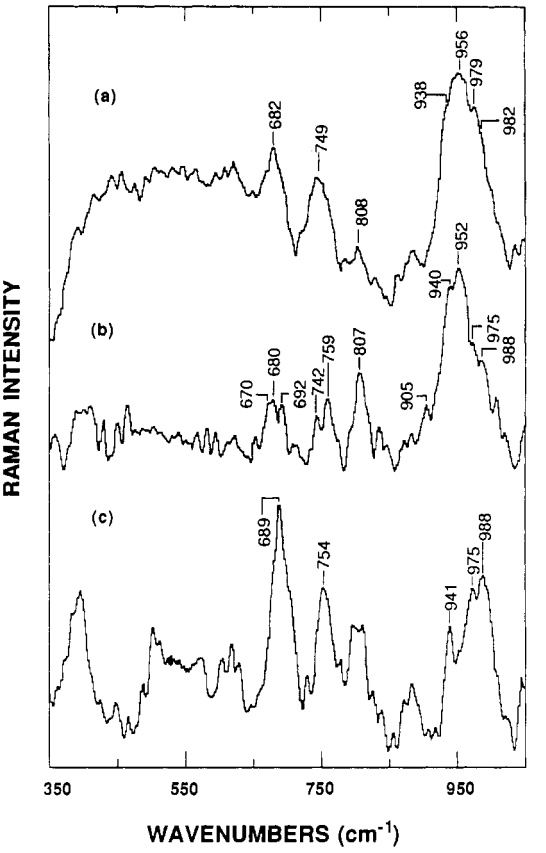

FIGURE 4: Raman spectra of (a) Zn_7-, (b) Cd_7-, and (c) apoMT-1 in deuterated 25 mM Tris buffer, pD 8.6 (a and b) and pD 1.7 (c). Experimental conditions as in Figure 3.

Both Zn_7- and Cd_7-MTs exhibit a split amide I band broader than that in apoMT, with peaks around 1650 and 1665 cm^{-1} (Figure 1a,b). The amide I band of the apoprotein is narrower and centered around 1676 cm^{-1} with shoulders around 1650 and 1665 cm^{-1} (Figure 1c). Deuteration appears to influence all three derivatives in a similar manner (Figure 2) and results in comparable amide I′ profiles.

The Raman spectral region spanning 1000–1800 cm^{-1} not only monitors the structural changes consequent to metal binding by apoMT but also highlights mutual differences between the two metal-bound forms. Thus, the amide III bands are collectively more intense in Zn_7-MT than in Cd_7-MT, although the general profile is nearly identical in the two cases. Similarly, the C–N stretching frequency region between 1000 and 1100 cm^{-1}, which is nearly as intense as the amide I in the apoprotein, falls successively following the respective incorporation of Zn (Figure 1a) and Cd (Figure 1b) ions. In the region between 1400 and 1500 cm^{-1}, Zn_7-MT and apoMT show comparable intensities, but Cd_7-MT is lower. One striking feature of this spectral region is the presence of a band of low intensity at 1532 cm^{-1} in Zn_7-MT and its near absence in Cd_7-MT and apoMT. This line is partly sensitive to deuteration, as shown in Figure 2a.

Figure 3 shows the Raman spectral features below 1000 cm^{-1} for Zn_7-MT (Figure 3a), Cd_7-MT (Figure 3b), and apoMT (Figure 3c). This region of the apoprotein spectrum is unexpectedly complicated by significant contributions from buffer peaks and poor scattering by the protein. Therefore, the only bands clearly assignable to the apoprotein are those at 659, 675, 752, and 941 cm^{-1}. Most of the other lines contain substantial contributions from Tris buffer at this low pH. In the holoMT spectra, a number of protein-specific lines are clearly discernible: In the C–S stretching region, Zn_7-MT shows a broad band centered around 680 cm^{-1}, which in Cd_7-MT is less intense, narrower, and split into two lines at 680 and 698 cm^{-1}. An unusually intense band near 760 cm^{-1} with shoulders around 780 and 802 cm^{-1} is present in both holoproteins. Between 850 and 1000 cm^{-1}, the metal-containing derivatives exhibit lines around 890 and 932 cm^{-1} and a doublet at 961 and 978 cm^{-1}, which is missing in apoMT. Scattering below 600 cm^{-1} arises predominantly from Tris buffer at pH 8.6 for Zn_7- and Cd_7-MTs and at pH 1.7 for apoMT. The effect of sample deuteration is shown in Figure 4, and all three spectra in deuterated buffer are marked by a substantial intensity increase in the region between 940 and 980 cm^{-1}. For the two holoproteins, there is also a marked drop in intensity at 760 cm^{-1}, whereas for apoMT the intensity of the line at 754 cm^{-1} is virtually unchanged. Between 650 and 700 cm^{-1}, the apoprotein shows significant intensity increase while this region is nearly unaltered in the holoproteins.

The infrared spectra of films of native (Cd_5,Zn_2)-MT and apoMT, obtained with ATR, are shown in Figure 5. Native MT (Figure 5a) is characterized by an amide I band at 1657 cm^{-1} and an amide II at 1528 cm^{-1}, both of which show virtually no splitting when compared to those in the Raman spectra (Figures 1 and 2). In the amide III region, two small bands of comparable intensity at 1240 and 1290 cm^{-1} are clearly distinguishable. In D_2O solution, however (data not shown), the amide I′ band of the native protein appears at 1643 cm^{-1}, with a strong shoulder around 1660 and weak shoulders at 1638 and 1685 cm^{-1}. ApoMT exhibits a closely similar IR profile in thin films, with the amide I and II bands at 1653 and 1530 cm^{-1}, respectively. In D_2O solution, the amide I′ is downshifted to 1647 cm^{-1}, with a prominent shoulder at 1675

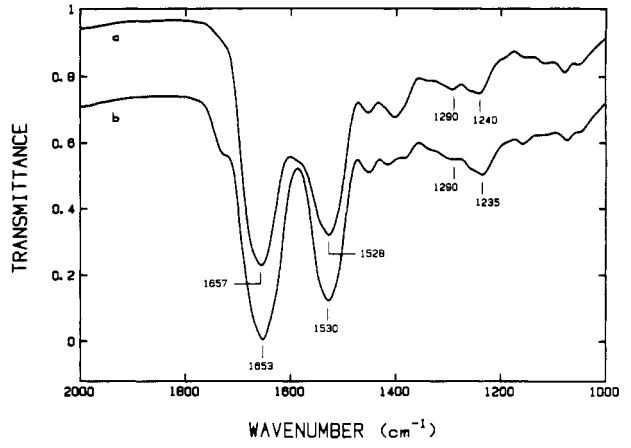

FIGURE 5: Infrared ATR spectra of (a) (Cd_5Zn_2)- and (b) apoMT-1 as films.

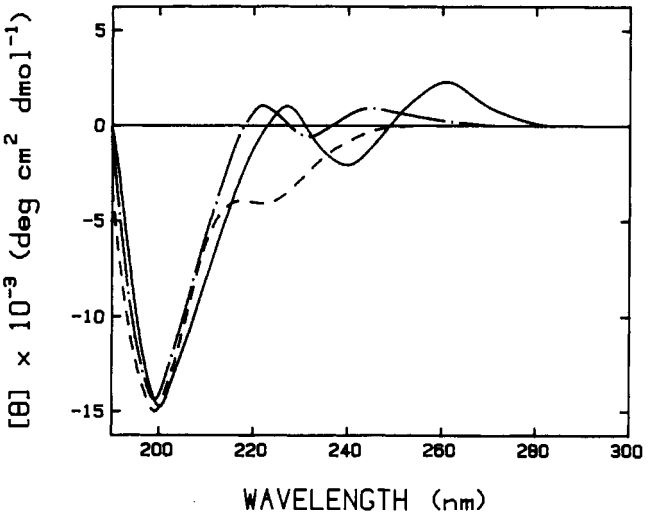

FIGURE 6: CD spectra of (a) Zn_7- (-·-), (b) Cd_7- (—), and (c) apoMT-1 (--). Spectra were measured in 25 mM Tris buffer at pH 8.6 (a and b) and in 0.02 M perchloric acid at pH 1.7 (c).

and a weak shoulder near 1638 cm^{-1}.

The spectropolarimetric properties of reconstituted zinc and cadmium MTs and apoMT are shown in Figure 6. The apoprotein is characterized by a large negative band at 199 nm with a negative shoulder at 222.5 nm. Analysis according to the method of Provencher and Glöckner (1981) yields a contribution of 6% α-helix, 18% β-sheet, 21% β-turn, and 55% unordered segments to the secondary structure of the metal-free protein. In contrast to the CD profile of the apoprotein, the holoMT spectra display positive and negative ellipticity bands between 210 and 300 nm, originating from metal–ligand charge-transfer transitions. These strongly mask the ellipticities arising solely from the $n-\pi^*$ and $\pi-\pi^*$ transitions of the amide group (Vašák & Kägi, 1983). Analysis of these spectra for secondary structural elements would thus yield erroneous results.

Discussion

The predominant contribution to the nonresonance Raman and IR spectra of a polypeptide chain stems from the several different normal vibrational modes of the backbone amide group and some amino acid side chains (Carey, 1982; Tu, 1982). The normal modes most relevant to structure elucidation are the amide I, III, and II bands, of which the former two are Raman active. The latter band is intense in the IR but is rarely seen in the Raman spectrum. Conventionally, the nonresonance Raman spectrum of a protein has been interpreted on the basis of the data on homopolymers representative of the α-helical, β-sheet, and disordered conformations. The detection and assignment of turns has, at best, been difficult because of the putative overlap of turn frequencies with the more commonly recognizable elements of secondary structure. Thus, the detailed normal-mode calculations for the three basic types of β-turns, i.e., I, II, and III and their mirror images, and several of their variants by essentially two groups have been a tremendous advantage in their identification in small peptides. Limited application to proteins has also been reported (Krimm, 1983).

On the basis of calculations on an alanyl tetrapeptide, Krimm and Bandekar (1980) first predicted high-frequency amide III modes ranging from 1290 to 1330 cm^{-1} to be diagnostic of β-turns. Since the amide III modes of the α-helical, β-sheet, and random conformations lie below 1300 cm^{-1}, this region was deemed best suited to detect the turn conformation. In contrast, the more recent calculations of Lagant et al. (1984a–c) predict the amide III mode of the β-turn to be around 1284 cm^{-1}, with varying contributions to the region between 1239 and 1284 cm^{-1} depending on the type of turn. In the case of MT, the Raman spectra of the two metal-containing derivatives (Figure 1a,b) show intense lines throughout the 1240–1330-cm^{-1} region. On the basis of the large intensity loss upon deuteration (Figure 2a,b), the Raman lines near 1240, 1252, 1285, 1296 (better resolved for Cd_7-MT), and 1310 cm^{-1} and shoulders above are all clearly attributable to the amide III mode. For native (Cd_5,Zn_2)-MT, the corresponding amide III region in the IR spectrum (Figure 5a), shows lines at 1240 and 1290 cm^{-1}. Evidently then, for the metal-containing MTs, the amide III lines near 1296 cm^{-1} and above in the Raman spectrum and at 1290 cm^{-1} in the IR spectrum are in good agreement with the calculated frequencies of Krimm and Bandekar (1980), for β-turns. However, as indicated by these authors, while these high-frequency modes are diagnostic of turns in general, they cannot be used to distinguish between them as they are not specific for turn type. This is better achieved by examining the scattering pattern below 1295 cm^{-1}, which reveals that the multiple amide III modes at 1240, 1252, 1285, and 1295 cm^{-1} in Zn_7- and Cd_7-MT correspond closely with those predicted for β-turns of type II or II′ by Lagant et al. (1984b). This is consistent with the 2D NMR data for Cd_7-MT in which predominantly turns of type II have been found (Wagner et al., 1986). Any nontrivial contribution from α-helical structures to the intensity of these amide III bands can be excluded, since no strong skeletal stretching mode appears between 900 and 950 cm^{-1} (Figure 3a,b), in Zn_7- and Cd_7-MTs. In a similar vein, the absence of a strong amide III line below 1240 cm^{-1} negates the presence of extended antiparallel β-sheet in holoMT. In view of the secondary structure predictions and the X-ray and 2D NMR data cited above, this is not a surprising result.

In apoMT, the intense lines between 1240 and 1280 cm^{-1}, by virtue of their sensitivity to deuteration, are also true amide III modes. Interestingly, the high-frequency modes near 1298 and 1310 cm^{-1}, in contrast to holoMTs, are not influenced by deuteration and hence cannot have any contribution from the NH in-plane bending mode. For apoMT therefore, the amide III frequencies are restricted to the lines near 1240, 1252, and 1285 cm^{-1}, with the high-frequency lines near 1300 and 1310 cm^{-1} most likely stemming from backbone skeletal vibrations. In the metal-free derivative therefore, the absence of true amide III modes beyond 1290 cm^{-1} argues against the presence of β-turns, although the partial loss of intensity at 1285 cm^{-1}

upon deuteration favors some, if minimal, contribution from turns to its secondary structure. Since, in general, randomly folded polypeptides exhibit amide III bands between 1240 and 1260 cm^{-1} (Frushour & Koenig, 1975), it follows that the intense lines below 1260 cm^{-1} in apoMT could originate from a disordered conformation. This assignment is substantiated by the CD spectral data shown in Figure 6.

The far-UV CD spectrum of apoMT (Figure 6c) is unlike any of the different classes of CD spectra calculated for β-turns (Woody, 1974) and is typical of polypeptides with predominantly disordered conformations (Chen et al., 1972). This is also evident from the analysis of the spectrum according to Provencher and Glöckner (1981), which yields 55% disordered, 21% β-turn, and 18% β-sheet with a negligibly small (6%) α-helical contribution. Accordingly, the assignment of the 1240–1260-cm^{-1} amide III lines in the Raman spectrum of apoMT to a random-coil conformation is justified, and the intensity around 1240 cm^{-1} possibly reflects the presence of about 18% β-sheet calculated from the CD data. As mentioned above (see Results), for the holoMTs, the substantial contribution of the ellipticities originating from the metal–ligand charge-transfer bands to the CD spectra below 300 nm undermine their use in an analogous analysis.

It thus follows that metal binding leads to a transition from a predominantly disordered conformation to one that is composed largely of turns and unordered segments. This is reflected in the decrease in intensity in the 1240–1260-cm^{-1} region and the appearance of true amide III modes above 1284 cm^{-1} for Cd_7- and Zn_7-MTs relative to the apoprotein and the near disappearance of the skeletal doublet found in apoMT between 1300 and 1310 cm^{-1}. This structural transition seems to favor the generation of type II β-turns or their close variants, a conclusion also reinforced by the vibrational pattern in the amide I region of the Raman spectrum discussed below.

The splitting pattern in the amide I band between 1600 and 1700 cm^{-1} is a function of the coupling between the various >C=O groups in the four-residue segment constituting a turn. This has been calculated in detail for all three major turn types and their mirror images at various values of the effective transition dipole moment (Krimm & Bandekar, 1980). The Raman spectra of the metal-bound MTs (Figure 1a,b) and the IR spectra in D_2O of the native MT (not shown) all exhibit split amide I and I′ frequencies at 1650 and 1666 cm^{-1} in the former and 1643 and 1660 cm^{-1} in the latter case. The close correspondence between the experimentally observed frequencies and those predicted at 1656 and 1666 cm^{-1} by Krimm and Bandekar (1980), for a type II β-turn with an effective transition moment μ_{eff} = 0.45 D, confirm the conclusions derived above from the collective vibrational spectral data in the amide III region. In addition, the amide I and I′ profiles of the spectra of the holoproteins also provide an indication that β-turns of type III (or 3_{10}-helical segments) may be present. This is suggested by the shoulders near 1630 and 1695 cm^{-1} better defined for Cd_7- than for Zn_7-MT and near 1638 and 1685 cm^{-1} in the IR spectrum in D_2O of (Cd_5,Zn_2)-MT (not shown), which are in excellent agreement with the theoretical predictions of Lagant et al. (1984b) at 1630, 1658, and 1697 cm^{-1} for type III turns. In the metal-free derivative (Figure 1c), supporting evidence for a disordered conformation inferred above is provided by the major amide I line at 1676 cm^{-1}, with the shoulders near 1650 and 1666 cm^{-1} hinting at the possible presence of residual turn structure. This could also be the source of the partial intensity of its amide III line at 1284 cm^{-1}. The intensification of the 1650-cm^{-1} line in the holoproteins and the opposing variation in the 1666- and 1676-cm^{-1} lines compared to apoMT are entirely compatible with the transition to type II β-turns accompanying metal binding.

From 600 to 1000 cm^{-1}, the Raman spectra of Cd- and Zn-MTs display novel features radically different from those of their metal-free counterpart (Figure 3). For reasons discussed above (see Results), relatively few lines in the apoMT spectrum are clearly assignable to the protein. Between 950 and 1000 cm^{-1}, the region attributed to backbone C–C–C and C–C–N stretching modes, a distinctive doublet is present in the holoMTs at 960 and 978 cm^{-1} but absent in the apoMT. This difference may be diagnostic of the manifestation of β-turns in the holoproteins, since predicted skeletal stretching modes of both type I and type III turns (Krimm & Bandekar, 1980) occur close to these values. Interestingly, no skeletal mode at 960 cm^{-1} is predicted for the type II β-turn by these authors. More importantly, the skeletal modes of β-turns in general seem to be shifted to higher frequencies with respect to those of the α-helix and random coil, which usually appear between 900 and 940 cm^{-1} (Frushour & Koenig, 1975). Thus, unordered segments in all three derivatives are the likely source of the weak lines between 900 and 940 cm^{-1}.

The region between 600 and 720 cm^{-1} typically arises from the C–S stretching modes of cysteinyl and methionyl residues (Carey, 1982; Tu, 1982). On the basis of model dialkyl disulfide data (Sugeta et al., 1972, 1973), the position of the C–S stretch has often been correlated with the geometry around the HC–CS bond. HoloMT totally lacks both S–S and free SH groups, and all cysteine sulfurs coordinated to the metals are either terminal or bridging ligands (Otvos & Armitage, 1980). The C–S stretching frequency in holoMT is additionally influenced by these constraints, which would alter the effective electron density around each sulfur atom. The splitting pattern in the C–S stretching region possibly reflects this and yields multiple frequencies for the bridging and terminally ligated sulfur atoms at lower and higher energies, respectively. Such an effect seems more pronounced for Cd_7- than for Zn_7-MT since the C–S region is a broad envelope in the latter and shows discrete lines in the former (Figure 3a,b). In contradiction to its predominantly random conformation, apoMT also shows a split C–S stretching frequency at 659 and 675 cm^{-1} (Figure 3c). However, the intense –SH stretch (not shown) in the apoMT is symmetrical and appears at 2575 cm^{-1}, a value typical of normal thiols (Tu, 1982).

The vibrational pattern from 720 to 820 cm^{-1} originates, in the absence of aromatic amino acid residues, chiefly from backbone skeletal bending modes and the out-of-plane bending modes of the amide group. The apoMT spectrum exhibits a strong line at 752 cm^{-1}. In the holoMTs, an intense line appears at 761 cm^{-1}, in addition to two new, weak lines near 782 and 802 cm^{-1}. Both the line at 761 cm^{-1} and the shoulder at 782 cm^{-1} in Zn_7- and Cd_7-MTs show appreciable loss in intensities following deuteration (Figure 4a,b), which implies that they could arise in part from the amide V or out-of-plane N–H bending mode. The region below 600 cm^{-1} does not, however, show a detectable increase in intensity corresponding to the N–H to N–D shift of the amide V mode. The deuteration-insensitive, residual scattering intensities at 749 and 808 cm^{-1} in Zn_7-MT and at 742, 759, and 806 cm^{-1} in Cd-MT could be a composite of the amide VI or >C=O out of plane bending (Harada et al., 1975) and skeletal N–C–C and C–N–C bending modes (Lagant et al., 1984a). The fact that the amide V mode is peculiar to metal-bound MTs is clearly demonstrated by the absence of a deuteration-sensitive com-

ponent to the line at 752 cm^{-1} in the apoprotein (Figures 3c and 4c). This line in apoMT possibly arises from the amide VI and skeletal bending modes alone. It is significant that our assignment of the lines at 761 and 782 cm^{-1} to the amide V modes in holoMT are in excellent agreement with those predicted at 767 and 784 cm^{-1} for a type III β-turn (or one turn of a 3_{10}-helix), by Lagant et al. (1984b). This region of the Raman spectrum of the holoMTs therefore offers conclusive evidence for the presence of a type III β-turn previously implied by the amide I splitting pattern (see discussion above). It must be pointed out that Krimm and Bandekar (1980) predict a rather wide spectral range (573–671 cm^{-1}) for a type III β-turn, which is in contradiction to our observed values. A 3_{10}-helical segment between S45 and C50 has recently been identified in the (Cd_5,Zn_2)-MT-2 from rat liver by X-ray crystallography (Furey et al., 1986). In the reconstituted rabbit liver Cd_7-MT-2, two such segments have been identified between A42–G47 and S58–A61 by 2D NMR studies (Wagner et al., 1986). It is also evident from our results that although the MT-1 used in these studies has been shown by HPLC analysis to be more heterogenous than MT-2 (Klauser et al., 1983), there is good agreement between our conclusions and those drawn from 2D NMR data on MT-2. This demonstrates that both isoforms exhibit essentially identical folding patterns.

With respect to the Raman spectral differences between the two holoMTs, the presence of a weak line at 1536 cm^{-1} in Zn_7-MT (Figure 1a) and its near absence in the Cd_7 derivative (Figure 1b) are immediately obvious. Its sensitivity to deuteration (Figure 2a) indicates that it stems at least in part from the amide II mode, which is generally detectable in the Raman spectrum only under resonance conditions (Harada et al., 1975). Since β-turns lack symmetry, however, the amide II mode should in principle also appear in the normal Raman spectrum (Krimm & Bandekar, 1980). Other differences are evident throughout the 1000–1700 cm^{-1} region for the holoproteins. These include differences in the relative intensities and widths of the various bands in the C–N stretching (1000–1100 cm^{-1}) and the COO^- stretching and CH_2– deformation (1350–1500 cm^{-1}) regions, and in the amide I and III bands. Qualitatively, such variations are to be expected in view of the differences in ionic size and polarizing abilities of the two metal ions (Aylett, 1979). In the native (Cd_5,Zn_2)-MT, X-ray crystal data have shown that the two zinc ions in the β-fragment are uniquely coordinated by two CXXC segments to the same metal (Furey et al., 1985). Thus, the local environment of the two Zn(II) ions is likely to be different from that of the remaining five Cd(II) ions. When these two zinc ions are replaced by Cd ions to yield a Cd_7-reconstituted MT, the backbone skeletal changes could conceivably be different from the case where the five Cd ions are replaced by zinc ions to yield reconstituted Zn_7-MT. The vibrational Raman spectrum, which is known to be highly sensitive to conformational changes, probably reflects this phenomenon. Whether these effects can be correlated to differences directly within the metal–thiolate clusters can only be ascertained by examining both the Raman and IR vibrational regions below 350 cm^{-1}, which are specific to metal–ligand stretching and cluster breathing modes (Haberkorn et al., 1976). Resonance Raman spectra in the metal–ligand vibrational region have been particularly useful in understanding various types of iron–sulfur clusters (Spiro et al., 1982).

It is important to mention here that the amide I band in the Raman spectra of several proteins has been quite successfully resolved to yield accurate estimates of secondary structural elements, in good agreement with X-ray data (Williams, 1983). Our analysis of the amide I band for the three MT derivatives according to the established methods of (i) Williams (1983) and (ii) Vogel (1985) led to values that differed not only mutually but also from the 2D NMR data. Thus, while the analysis according to Williams (1983) yielded on an average 25–35% α-helix, 35–40% β-sheet, 12–15% β-turn, and 10–15% undefined structure, that of Vogel (1985) yielded 4–10% α-helix, 60–65% β-sheet, 20% β-turn, and 10% undefined components, either of which is in contradiction with secondary structure predictions and X-ray and NMR results for MT. This is also true of the amide I′ mode in the IR spectra, which when analyzed according to the method of Eckert et al. (1977) yielded erroneously high values for extended sheet structure in holoMT. We therefore suggest that caution be exercised in such analyses for proteins with atypical structures like MT, since the existing basis set of proteins may not be strictly applicable.

Conclusions

Our Raman spectral data on metal-containing MT-1 confirm many of the theoretical predictions reported for the normal modes of β-turns. The presence of intense amide III bands above 1290 cm^{-1} is in good agreement with those predicted by Krimm and Bandekar (1980) and is unequivocal evidence for the presence of β-turns. However, in contradiction to their prediction and in agreement with those of Lagant et al. (1984b), strong support for the presence of turns of type II is obtained from the amide III bands below 1290 cm^{-1}. While this may be true for MTs that have independently been shown to consist mainly of turns, such an assignment would be more involved for other proteins due to overlapping amide III modes from the α-helix, β-sheet, and disordered structures. Thus, we tend to agree with the former group that, in general, only high-frequency amide III modes can be unambiguously diagnostic of turns, although the turn type cannot be distinguished from these modes alone.

The splitting pattern in the amide I region of the holoproteins provides supporting evidence for the type II turn and indicates possible contribution from a type III turn. This is reinforced by the presence of the amide V modes at 761 and 782 cm^{-1}, which closely correspond to the predicted frequencies of Lagant et al. (1984b). The data presented here also highlight the potential of the Raman spectral region below 1000 cm^{-1} in monitoring conformational changes in an atypical metalloprotein like MT. This is reflected in the appearance of an amide V mode and several backbone skeletal modes consequent to metal incorporation into apoMT.

Acknowledgments

We are indebted to Drs. R. W. Williams and H. Vogel for the analyses of the Raman spectra in the amide I region, to Dr. U. P. Fringeli and M. Fringeli for assistance in measuring IR ATR spectra, and to M. Sutter for the isolation of MT.

References

Aylett, B. J. (1979) in *The Chemistry, Biochemistry and Biology of Cadmium* (Webb, M., Ed.) pp 1–43, Elsevier/North-Holland, New York.

Bandekar, J., & Krimm, S. (1979) *Proc. Natl. Acad. Sci. U.S.A. 76*, 774–777.

Bandekar, J., Evans, D. J., Krimm, S., Leach, S. J., Lee, S., Mcquie, J. R., Minasian, E., Nemethy, G., Pottle, M. S., Scheraga, H. A., Stimson, E. R., & Woody, R. W. (1982)

Int. J. Pept. Protein Res. 19, 187–205.
Boulanger, Y., Goodman, C. M., Forte, C. P., Fesik, S. W., & Armitage, I. M. (1983) *Proc. Natl. Acad. Sci. U.S.A. 80*, 1501–1505.
Braun, W., Wagner, G., Wörgötter, E., Vašák, M., Kägi, J. H. R., & Wüthrich, K. (1986) *J. Mol. Biol. 187*, 125–129.
Carey, P. R. (1982) *Biochemical Applications of Raman and Resonance Raman Spectroscopies*, Academic, New York.
Chen, Y. H., Yang, J. T., & Martinez, H. M. (1972) *Biochemistry 11*, 4120–4131.
Eckert, K., Grosse, R., Malur, J., & Repke, K. R. H. (1977) *Biopolymers 16*, 2549–2563.
Frushour, B. G., & Koenig, J. L. (1975) *Adv. Infrared Raman Spectrosc. 1*, 35–97.
Furey, W. F., Robbins, A. H., Clancy, L. L., Winge, D. R., Wang, B. C., & Stout, C. D. (1986) *Science (Washington, D.C.) 231*, 704–710.
Gilg, D. E. O. (1985) Ph.D. Thesis, University of Zürich, Switzerland.
Haberkorn, R. A., Que, L., Jr., Gillum, W. O., Holm, R. H., Liu, C. S., & Lord, R. C. (1976) *Inorg. Chem. 15*, 2408–2414.
Harada, I., Sugawara, Y., Matsuura, H., & Shimanouchi, T. (1975) *J. Raman Spectrosc. 4*, 91–98.
Hollosi, M., Kawai, M., & Fasman, G. D. (1985) *Biopolymers 24*, 211–242.
Kägi, J. H. R., Vašák, M., Lerch, K., Gilg, D. E. O., Hunziker, P., Bernhard, W. R., & Good, M. (1984) *EHP, Environ. Health Perspect. 54*, 93–103.
Kimura, M., Otaki, N., & Imano, M. (1979) in *Metallothioneins* (Kägi, J. H. R., & Nordberg, M., Eds.) pp 163–168, Birkhäuser, Basel.
Klauser, S., Kägi, J. H. R., & Wilson, K. J. (1983) *Biochem. J. 209*, 71–80.
Krimm, S. (1983) *Biopolymers 22*, 217–225.
Krimm, S., & Bandekar, J. (1980) *Biopolymers 19*, 1–29.
Lagant, P., Vergoten, G., Fleury, G., & Loucheux-Lefebvre, M. (1984a) *Eur. J. Biochem. 139*, 137–148.
Lagant, P., Vergoten, G., Fleury, G., & Loucheux-Lefebvre, M. (1984b) *Eur. J. Biochem. 139*, 149–154.
Lagant, P., Vergoten, G., Fleury, G., & Loucheux-Lefebvre, M. (1984c) *J. Raman Spectrosc. 15*, 421–423.
Nordberg, M., & Kojima, Y. (1979) in *Metallothionein* (Kägi, J. H. R., & Nordberg, M., Eds.) pp 41–116, Birkhäuser, Basel.
Otvos, J. D., & Armitage, I. M. (1980) *Proc. Natl. Acad. Sci. U.S.A. 77*, 7094–7098.
Provencher, S. W., & Glöckner, J. (1981) *Biochemistry 20*, 33–37.
Richardson, J. S. (1981) *Adv. Protein Chem. 34*, 167–339.
Rose, G. D., Gierasch, L. M., & Smith, J. A. (1985) *Adv. Protein Chem. 37*, 1–109.
Spiro, T. G., Hare, J., Yachandra, V., Gewirth, A., Johnson, M. K., & Remsen, E. (1982) *Met. Ions Biol. 4*, 407–423.
Sugeta, H., Go, A., & Miyazawa, T. (1972) *Chem. Lett.*, 83–86.
Sugeta, H., Go, A., & Miyazawa, T. (1973) *Bull. Chem. Soc. Jpn. 46*, 3407–3411.
Tu, A. T. (1982) *Raman Spectroscopy in Biology*, Wiley, New York.
Vašák, M., & Kägi, J. H. R. (1983) *Met. Ions Biol. Syst. 15*, 213–273.
Venkatachalam, C. M. (1968) *Biopolymers 6*, 1425–1436.
Vogel, H., Wright, J. K., & Jähnig, F. (1985) *EMBO J. 4*, 3625–3631.
Wagner, G., Neuhaus, D., Wörgötter, E., Vašák, M., Kägi, J. H. R., & Wüthrich, K. (1986) *J. Mol. Biol. 187*, 131–135.
Williams, R. W. (1983) *J. Mol. Biol. 166*, 581–603.
Woody, R. W. (1974) in *Peptides, Polypeptides and Proteins* (Blout, E. R., Bovey, F. A., Lotan, N., & Goodman, M., Eds.) pp 338–360, Wiley, New York.